Journal of Applied Polymer Science

Fracture toughness of carbon fiber/polyether ether ketone composites manufactured by autoclave and laser-assisted automated tape placement

Dipa Ray, Anthony J. Comer, John Lyons, Winifred Obande, David Jones, Ronan M. O. Higgins, Michael A. McCarthy

Department of Mechanical, Aeronautical and Biomedical Engineering, Irish Centre for Composites Research (ICOMP), Materials and Surface Science Institute, University of Limerick, Limerick, Ireland

Correspondence to: R. M. O. Higgins (E-mail: ronan.ohiggins@ul.ie)

ABSTRACT: A comparative study is presented on the fracture toughness of carbon fiber/PEEK composites manufactured by autoclave and laser-assisted automated tape placement (LATP). Formation of a good inter-laminar bond is always a concern in ATP due to the short time available for intimate contact development and polymer healing, yet our double cantilever beam (DCB) tests reveal 60–80% higher Mode I fracture toughness for the LATP processed specimens than for the autoclave processed specimens. This magnitude of difference was unexpected, so specimens were further examined via differential scanning calorimetry, dynamic mechanical analysis, nano-indentation, and scanning electron microscopy. The results indicate that the LATP process has been very effective in heating and consolidating the surface of plies, creating an excellent bond. However, it has been less effective in processing the interior of plies, where a low crystallinity and poor fiber–matrix bonding are evident. The higher fracture toughness of the LATP processed specimens is also not solely due to a better bond, but is partially due to significant plastic deformation in the interior of plies during the DCB test. The findings indicate there is still considerable scope for optimizing the laser-assisted ATP process, before the optimum balance between strength and toughness is achieved at favorable lay-down speeds. © 2014 Wiley Periodicals, Inc. J. Appl. Polym. Sci. **2015**, *132*, 41643.

KEYWORDS: composites; morphology; structure; property relations

Received 1 August 2014; accepted 12 October 2014

DOI: 10.1002/app.41643

INTRODUCTION

Carbon fiber/poly(ether ether ketone) (CF/PEEK) composites are of major interest for high performance composite applications, and a wide range of manufacturing techniques can be used to produce high quality CF/PEEK composite laminates. Autoclave processing produces laminates with optimum mechanical properties, against which other manufacturing techniques can be compared. During the process CF/PEEK tapes are heated above the melting point of PEEK under pressure to ensure intimate contact between plies, followed by cooling at a controlled and relatively slow cooling rate, ensuring optimum crystallinity. However, while this technique produces excellent structures, it is relatively expensive in terms of labor, energy, consumables, and time.

A promising emerging technique is automated tape placement (ATP) which combines high productivity with an ability to deliver large, complex-geometry, composite parts.[1,2] In this process, the surfaces of two tapes are melted in a few seconds by the application of a heat source such as laser, infra-red, or hot gas, and consolidated *in situ* by application of pressure with a roller. Here, both the heating and cooling take place at a very fast rate, and pressure is lower than in an autoclave and applied over a very short time.[3,4] This is entirely different to the conditions in autoclave processing, and attaining autoclave-level mechanical properties is extremely challenging.

The Irish Centre for Composites Research (IComp) at the University of Limerick has recently installed a laser-assisted ATP (LATP) machine (Figure 1). As the application of lasers in tape placement is relatively new, and laser heating has some distinct differences from other forms of heating such as hot gas or infra-red heating,[5] it is important to understand how the LATP process influences the morphology development and consequent mechanical properties in CF/PEEK composites in comparison to well-consolidated autoclaved laminates. With such understanding process improvements can be implemented.

Formation of a good inter-laminar bond is always one of the chief concerns in ATP processing due to the short time available for intimate contact development and polymer healing

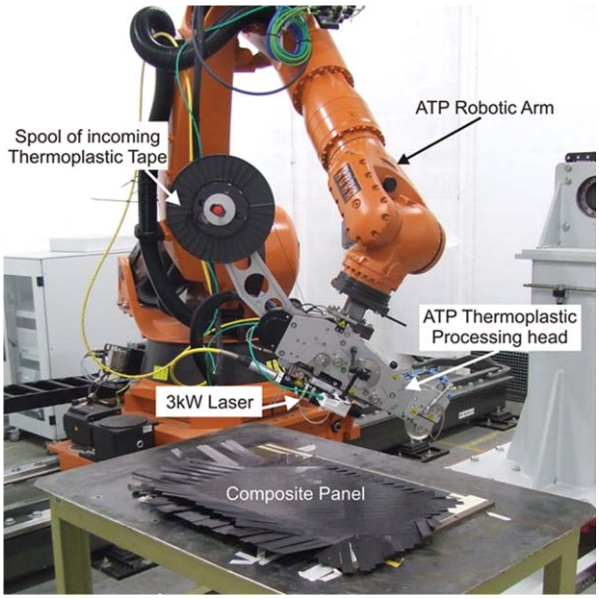

Figure 1. The laser assisted automated tape laying (LATP) machine. [Color figure can be viewed in the online issue, which is available at wileyonlinelibrary.com.]

(diffusion of polymer chains across the interface). As a result, a number of authors have developed quite detailed models of intimate contact formation and polymer healing during the ATP process.[6–10] In this article, we thus focus on the interlaminar behavior, in particular the fracture toughness of samples made by LATP and autoclave, and the processing variables affecting it.

It is well known that processing parameters control the final properties of consolidated thermoplastic laminates, especially when using semi-crystalline matrices like PEEK. The manufacturing technique influences the flow of the matrix during processing and the formation of crystalline phases, thus controlling the microstructure development, matrix ductility, and the fiber/matrix interfacial bonding. In the composite, a strong interaction exists between the stiff reinforcement fibers and the matrix which leads to a non-uniform crystalline morphology. Thermal stresses are also generated at the fiber/matrix interphase and mechanical restraints are introduced by the fibers. All these factors affect the development of the plastic zone ahead of a propagating crack and hence influence the overall fracture toughness of the composite. Because of the very different temperature and pressure conditions during autoclave and LATP processing, we can expect major differences in microstructure and hence fracture toughness.

Several researchers have examined the influence of CF/PEEK processing conditions on the fracture toughness, or factors which affect the fracture toughness such as crystallinity and fiber–matrix adhesion. Gao and Kim[11] manufactured composites with unidirectional CF/PEEK prepreg tapes and investigated the effect of cooling rate (between 1 and 180°C/min) on the interlaminar fracture toughness. They found that the propagation values of Mode I and II interlaminar fracture toughness increased with faster cooling rates, which they attributed to decreased crystallinity and hence enhanced matrix ductility at more rapid cooling rates. They stated that the cooling rate dependency of interlaminar fracture toughness is the result of complex interactions between two important properties, namely the matrix ductility and fiber–matrix interface bond strength. These two properties varied in a totally opposite manner with cooling rate through its effect on crystallinity: matrix ductility varied in direct proportion to cooling rate, while the converse was true for interface bond strength. The extent of plastic deformation of the PEEK matrix contributed a predominant part to composite toughness, while an adequate interface bond was found to be required to allow matrix deformation to take place to a full degree. In a separate paper, Gao and Kim[12] focused on fiber/matrix interfacial bond strength in carbon fiber/PEEK and found it in decreased substantially with faster cooling. Their tests on neat PEEK resin indicated that faster cooling resulted in reduced tensile strength and elastic modulus, but increased ductility, which they attributed to the effect of cooling rate on crystallinity and spherulite size. They stated that the improvement of crystalline perfection and flattened lamella chains with high crystallinity at the interphase region were mainly responsible for the strong fiber/matrix bond in composites processed at a low cooling rates. The same authors also studied the effect of cooling rate on the impact performance of carbon fiber/PEEK composites.[13] They stated that the higher matrix ductility and mode II interlaminar fracture toughness of fast-cooled carbon/PEEK composites resulted in higher damage resistance and damage tolerance in low-energy impact. They also stated that slow cooling improved both the fiber/matrix interfacial bond strength and strength/stiffness of PEEK matrix, resulting in high strength and modulus of the composite. Conversely, fast cooling enhanced the ductility of PEEK matrix, which in turn gave rise to high interlaminar fracture toughness and impact damage resistance of the composite. They thus concluded that desired properties can be tailored by selecting different processing conditions.

Li *et al.*[14] studied the influence of processing conditions on the morphology, interfacial interaction, and shear modulus of short-carbon-fiber reinforced PEEK composites. They concluded that melt residence time significantly influenced the interaction between PEEK crystallites and the carbon fibers which again controlled the fiber/matrix interfacial properties. Vu-Khanh and Frikha[15] also investigated the effect of processing on morphology, interface, and delamination in CF/PEEK composites. They stated that Mode-I delamination energy was controlled by matrix properties, whereas Mode-II was more dependent on fiber/matrix adhesion. They observed that higher crystallinity at low cooling rates resulted in a slight decrease in the Mode-I delamination energy. Crick *et al.*[16] examined in great detail the stable and unstable crack propagation areas of double cantilever beam (DCB) specimen fracture surfaces by scanning electron microscopy, and observed that polymer ductility differed in these regions. The PEEK spherulites were seen to nucleate from the fiber surfaces. By measuring the deformation zones they reported that the volume of the polymer in which the energy can be absorbed extends considerably beyond the inter-fiber or interlaminar distances.

In summary, it appears, especially from the work of Gao and Kim,[11–13] that high cooling rates can be advantageous for fracture toughness, due to increased polymer ductility. However,

Process Parameter	
Vacuum Level	900 mBar min
Heat-up Rate	3 °C/min
Dwell Temperature	375 °C
Pressure Ramp Rate	500 kPa/min
Dwell Pressure	7 Bar
Dwell Duration	20 min
Cool Down Rate	2 °C/min

Figure 2. Autoclave curing cycle and process parameters. [Color figure can be viewed in the online issue, which is available at wileyonlinelibrary.com.]

the work in Refs. 11–13 examined cooling rates of between 1 and 180°C/min, which is much lower than in the LATP process, where cooling rates are in excess of 333°C/s.[17] In addition, leveraging the advantage of a ductile matrix in a fracture toughness test, presupposes the formation of a good interlaminar bond. This was assured in Refs. 11–13, as the laminates were pressed in a mould at 400°C for 30 min, allowing plenty of time for intimate contact development and polymer diffusion across the ply interfaces, whereas no such assurance exists in the LATP process, where the pressure is applied for only 1–2 s at most. Finally, Gao and Kim[11] state that an adequate fiber/matrix bond is required to allow matrix deformation to take place to a full degree in the fracture toughness test, but also state that fiber–matrix bonding deteriorates at high cooling rates. Thus, it is unclear from the literature what level of fracture toughness can be expected from the LATP process.

In this study, a comparative analysis has been performed between the properties of CF/PEEK laminates manufactured by autoclave and LATP. The Mode-I fracture toughness was investigated through DCB tests and the fracture surfaces were analyzed with scanning electron microscopy (SEM). The composites were also subjected to differential scanning calorimetry (DSC) to investigate their level of crystallinity, while dynamic mechanical analysis (DMA) was used to measure the damping behavior. A nano-indentation technique was also adopted to measure the matrix modulus and hardness. From all this, a structure–property correlation was established, which gives insight into the influence of LATP and autoclave manufacturing techniques on the fracture toughness of CF/PEEK composites.

EXPERIMENTAL

Materials

The materials used were CF/PEEK prepreg tapes (T 60% IM7/PEEK-150) from Suprem (Switzerland). Conventional wide tapes (150 mm wide) were used for autoclave processing, while ATP grade tapes (12 mm wide) were used for LATP processing.

Manufacturing

For the autoclave processed specimens, flat $[0]_{30}$ laminates were laid up by hand and cured in an autoclave using standard autoclave manufacturing procedures. A high temperature polyimide vacuum bag was sealed to a flat steel tool plate using high-temperature sealant tape and a steel frame. A high-temperature breather was used to provide a vacuum path between the upper surface of the panels and the vacuum ports (evacuation and monitor ports). A slow cooling rate (2°C/min) was maintained during the cooling cycle, with the aim of achieving the recommended high PEEK crystallinity (~35%) for good mechanical properties.[18] The autoclave curing cycle and process parameters are shown in Figure 2.

Flat $[0^\circ]_{30}$ laminates were also manufactured with the narrow tape using an LATP head (AFPT, GmbH), attached to a robot arm (Kuka, KR240 L210-2). The tape head consists of: (i) an optical system connected to a remotely located 3 kW diode-laser heat source (wavelength, $\lambda \sim 1020$ nm), (ii) a tape feed, guidance, tensioning, and cutting system, (iii) a consolidation roller (outside diameter 80 mm), and (iv) a thermal camera. The laser beam is spread through optics to provide a range of spot sizes at the nip point depending on the focal length of the optic. With current optics (200 mm and 250 mm), the machine can process tape widths between 6 and 25 mm and the distribution of the beam can be biased towards the incoming tape or the substrate. Two types of consolidation rollers can currently be used on the system: rigid steel or conformable silicone. The consolidation roller is pressed onto the substrate by a pneumatic cylinder and is cooled either internally (steel roller) or externally (silicone roller) using compressed air to prevent the tape adhering to the roller during processing. The system is contained within an enclosure which is inaccessible during operation to prevent operator exposure to the laser. The process is monitored remotely by CCTV.

In the LATP process, there are many processing variables that must be controlled including: (a) laser power, (b) laser angle, (c) roller pressure, (d) tool temperature, (e) lay-down speed, and (f) roller cooling level. For this study, the processing parameters were chosen based on trials performed by the tape head manufacturer and are listed in Table I. There will be a huge scope of research in optimizing these process parameters in the future. The machine was operated in closed loop control, that is, the laser energy is governed by the difference in temperature between the set-point and the feedback measurements from the thermal camera. The thermal camera tends to overestimate the temperature at the nip point, as the material enters a

Table I. Laser ATP Processing Parameters Used for Manufacturing DCB Panel

	DCB panel
Lay-up	$[0°]_{30}$
Lay-down speed	8 m/min
Laser power (first ply)	1350 W
Tool temperature	150°C
Roller material	Silicone
Roller pressure[a]	1.2 Bar

[a] Roller is actuated via a pneumatic piston. Pressure indicated is the air pressure in the piston.

region which is shadowed relative to the laser before reaching the nip point. Thus, the set-point temperature is generally set somewhat above the desired surface temperature at the nip point. The lay-down speed of 8 m/min was chosen to allow comparison of results with other ATP processing techniques from the literature. Although the LATP machine is capable of higher speeds, this is considered to be at the upper effective speed range of typical gas-assisted ATP processes. A schematic diagram showing the LATP process is given in Figure 3.

Characterization

DCB Tests. The Mode-I interlaminar fracture toughness of the autoclaved and ATP-made samples was investigated by DCB tests, performed in accordance with ASTM D5528.[19] Five DCB specimens were extracted and tested from both of the laminates. The nominal dimensions of the DCB specimens were 150 mm × 25 mm × 4 mm with a $[0]_{30}$ lay-up. Both sides of the test specimens were coated with a thin layer of Tipp-Ex correction fluid from the end of the PTFE insert, and vertical lines were drawn prior to testing to help with crack length measurement. Loading blocks were used to apply the load during testing, which was performed using a multi-purpose Tinius Olsen machine. The specimens were mounted and subsequently loaded at a constant rate of 3 mm/min. A digital camera (Figure 4) was used to record the crack growth and the digital images were subsequently used to measure the crack length.

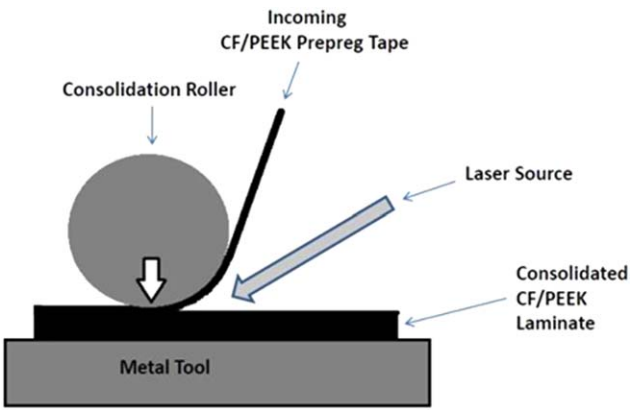

Figure 3. A schematic diagram of automated tape placement (ATP). [Color figure can be viewed in the online issue, which is available at wileyonlinelibrary.com.]

DSC Analysis. DSC was performed to evaluate the thermal properties of autoclaved and LATP-manufactured laminates. Specimens of approximately 10 mg were analyzed at a heating rate of 10°C/min from 30 to 375°C with an Elmer Pyris 1 DSC machine (Perkin).

Dynamic Mechanical Analysis. DMA was conducted with a TA Instruments DMA Q800 using the three-point bend clamp over a temperature range between 30 and 250°C with a temperature increase rate of 5°C/min. An amplitude of 10 μm was applied at a fixed frequency of 1 Hz.

Nano-Indentation. Nano-indentation experiments were performed on cross sections of the composite samples with an Agilent Nano-indenter G200 with a Berkovich indenter tip, which includes a continuous stiffness measurement (CSM) system. The main objective was to determine the difference in modulus and hardness of the PEEK matrix in the autoclave and LATP processed laminates, which resulted from the combined effect of variations in matrix crystallinity and fiber/matrix bonding occurring in the two processes. Laminate cross sections were selected for the nano-indentation study rather than the surface to get an insight into the consolidation quality through the thickness. The third ply from the top surface was chosen for nano-indentation in both the samples. A series of indentations were performed in resin pockets seen in the intra-ply regions. A fixed indentation depth of 2 μm was set, and the average elastic modulus and hardness values were calculated by standard methods from fifteen indentations.

Scanning Electron Microscopy of DCB Specimens. The fracture surfaces obtained from the DCB tests were examined using a Hitachi SU-70 scanning electron microscope (SEM). Prior to analysis, the samples were coated with a thin layer of gold, using an EMITech sputter coater for 30 s, to prevent charging of the specimens. An acceleration voltage of 10 kV was used. Some of the samples were mounted, ground, and polished, prior to gold coating. All images were taken at approximately 25 mm from the point of crack initiation in the DCB tests.

RESULTS

DCB Results

In all the DCB tests (autoclaved and LATP samples), stick-slip behavior was evident in the load–deflection curves, indicating regions of brittle crack propagation on the crack plane interspersed with regions of stable crack growth. The crack initiation and arrest loads were, however, significantly higher in the LATP samples. Visual inspection of the crack surface of the autoclaved specimens revealed light gray zones for the stable or slow crack growth areas, while the unstable or brittle crack growth areas appeared much darker [Figure 5(a)]. The LATP specimens also exhibited stable and unstable crack growth but, unlike the autoclaved specimens, no alternative light and dark zones were evident on the crack plane, which was mostly uniform throughout [Figure 5(b)].

The fracture toughness values at the crack initiation and arrest points were calculated using simple beam theory and are given in Table II. Fracture toughness was measured in the form of critical strain energy release rate (G_{IC}, kJ/m^2). The G_{IC}

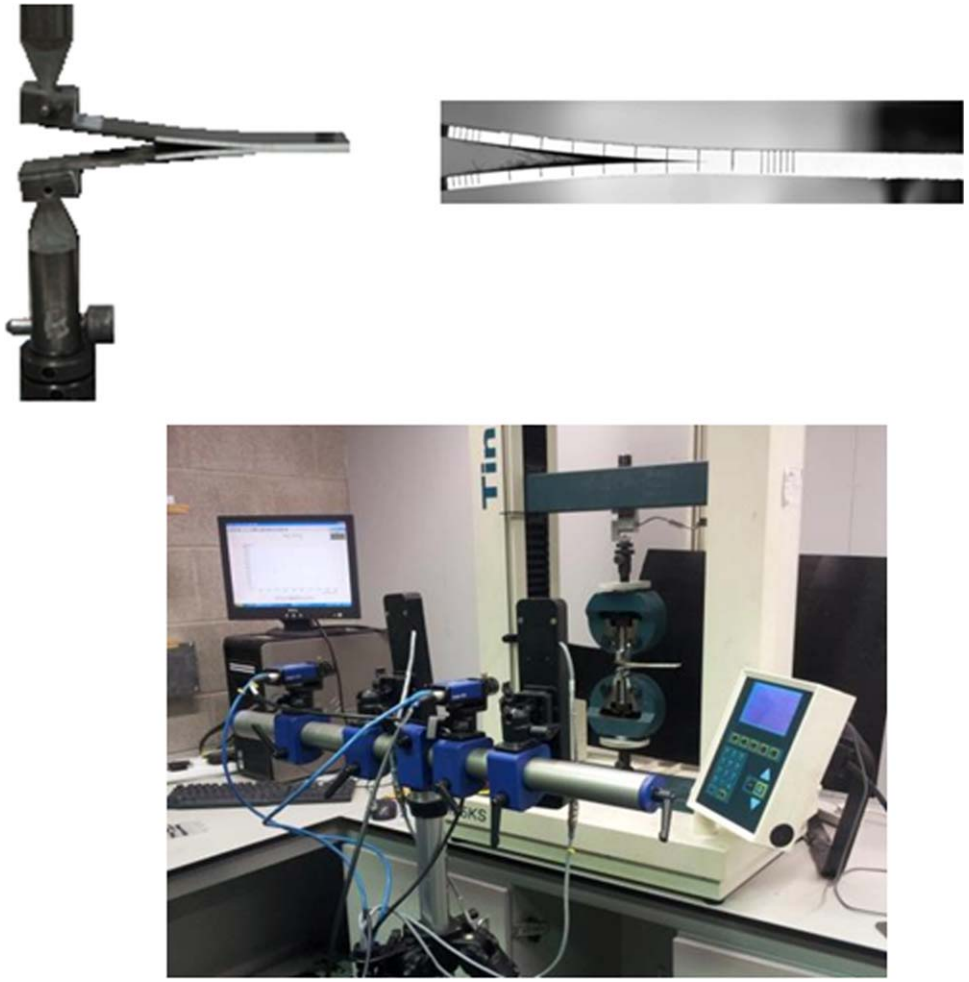

Figure 4. DCB test set up and camera. [Color figure can be viewed in the online issue, which is available at wileyonlinelibrary.com.]

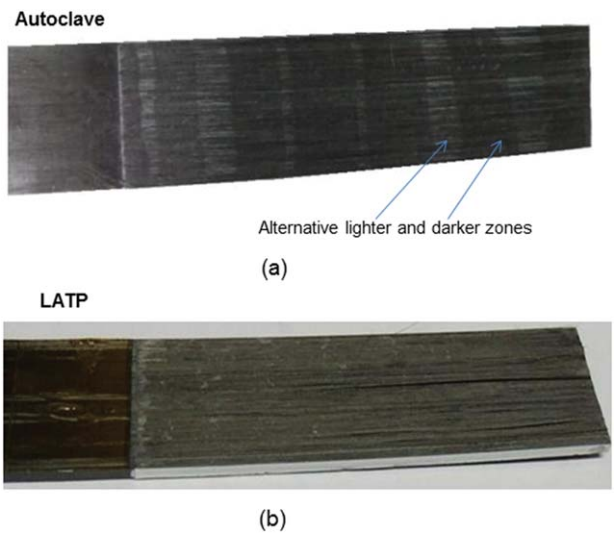

Figure 5. DCB fracture surfaces of (a) autoclave and (b) LATP samples. [Color figure can be viewed in the online issue, which is available at wileyonlinelibrary.com.]

(initiation) values were 1.32 kJ/m^2 and 2.15 kJ/m^2 for autoclaved and LATP-made samples, respectively (63% higher for LATP), while the G_{IC} (arrest) values were 0.92 kJ/m^2 and 1.67 kJ/m^2 for autoclaved and LATP-made samples, respectively (81% higher for LATP). The higher Mode I fracture toughness of the ATP-made samples relative to the autoclaved samples is not wholly unexpected, given previous findings that faster cooling rates lead to lower crystallinity and increased fracture toughness (albeit at much lower cooling rates).[11–13,15] It indicates a high quality inter-laminar bond has been formed despite the very short time available for intimate contact development and polymer diffusion. However, the magnitude of the difference between the fracture toughness of the autoclave and LATP processed samples came as a surprise, and the reasons for this are investigated further below.

The values obtained in this study are in the same range as G_{IC} values of CF/PEEK composites reported by other researchers. Vu-Khanh and Frikha[15] reported a G_{IC} value of 1.5–1.6 kJ/m^2 for CF/PEEK composites, compression-moulded at a cooling rate of 1°C/min. Gao and Kim[12] found G_{IC} values varied

Table II. DCB Results for Suprem CF/PEEK Material

Sample type	[a]G_{IC} initiation (kJ/m^2)	[a]G_{IC} arrest (kJ/m^2)
Autoclave	1.32	0.92
LATP	2.15	1.67

[a] Each G_{IC} value is a mean of five samples. For each sample, a mean G_{IC} value was obtained from approximately 10 points of initiation and arrest.

between 1.2 and 2.5 kJ/m^2 at a cooling rate of 1°C/min for the same combination of carbon fiber and PEEK matrix.

DSC Results

The crystallinity of the autoclave and LATP processed samples was measured using DSC; the following equation was used to calculate the degree of crystallinity (X),

$$X = \frac{\Delta H_m}{\Delta H_f (1-\alpha)}, \quad (1)$$

where ΔH_m is the enthalpy of fusion at the melting point as measured by the area under the endothermic peak; ΔH_f is the enthalpy of fusion of fully crystalline PEEK, which is taken to be 130 J/g,[20] and α is the weight fraction of fiber present in the composite. The DSC results are shown in Table III. The crystallinity was very high (42%) for the autoclave sample (a little higher than planned) while for the LATP sample, the crystallinity was just 17.6%. In the autoclave, the PEEK matrix is fully melted and re-solidified at a controlled, slow cooling rate of 2°C/min. But in the LATP process, the tape surface melts in a few seconds and re-solidifies under normal ambient conditions at a much faster rate.[3,4] It is already known that there is an increase in the crystalline mass fraction of PEEK if it is repeatedly heated above its T_g.[21] When a 30 ply laminate is manufactured by LATP, a few plies underneath the laser heated top surface undergo re-heating above the T_g, so can be expected to experience cold crystallization with a subsequent increase in the crystallinity of the finished product.[17] The measured crystallinity in the LATP laminate (17.6%) thus combines the effects from the laser heating, followed by rapid cooling and then cold crystallization experienced when subsequent layers are laid down, but is still very low.

DMA Results

DMA of autoclave and LATP processed laminates was performed to evaluate their mechanical properties under dynamic loading conditions as a function of temperature. The matrix morphology and the fiber/matrix interfacial bonding directly influence the dynamic mechanical behavior of the composites. The storage modulus of the LATP samples at room temperature was lower than that of the autoclaved samples [Figure 6(a)],

Table III. DSC Results for Suprem CF/PEEK Material

		Melting peak (°C)		
Sample type	T_g (°C)	Temp (°C)	Enthalpy (J/g)	%Crystallinity
Autoclave (30 ply)	153	345	18.4	42
LATP (30 ply)	140	346	7.5	17.6

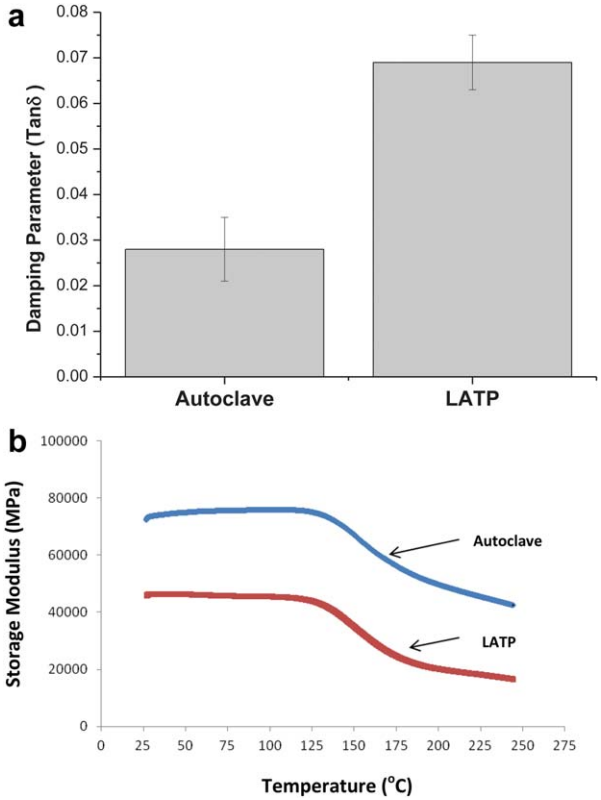

Figure 6. (a) Variation of storage modulus of autoclave and LATP laminates as a function of temperature. (b) Damping parameter of autoclave and LATP laminates. [Color figure can be viewed in the online issue, which is available at wileyonlinelibrary.com.]

while the damping parameter was much higher [Figure 6(b)]. Damping parameter reported here is the tan δ value from the peak of the tan δ versus temperature curve. These findings corroborate well with the crystallinity values reported in the previous section.

Nano-Indentation Results

A series of nano-indentations were performed in intra-ply resin pockets in both autoclaved and LATP-made samples in an attempt to determine the mechanical properties of the matrix constituent. A typical indentation in a resin pocket is shown in Figure 7 and the variation of elastic modulus with penetration depth is shown in Figure 8. The continuous stiffness measurement (CSM) results showed a plateau in the modulus values at low penetration depths up to 500 nm and beyond that, the modulus increased sharply (Figure 8) indicating that the presence of fibers had a strong influence on the resin deformation behavior at large penetration depths. These findings are in agreement with previous work which showed that the load-displacement data from nano-indentation tests performed in the resin region of a fibrous composite can be influenced by the reinforcing effect of the surrounding fibers.[22,23] As the elastic modulus was found to be very consistent for all indents in several different regions of the cross-section of LATP samples for penetration depths of 200–400 nm, and was also consistent (at a higher value) for autoclaved samples, this indicated that behavior over this range of penetration was a good measure of

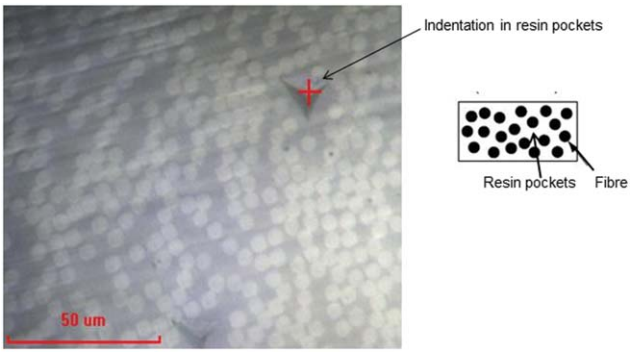

Figure 7. Indentation in a resin pocket. [Color figure can be viewed in the online issue, which is available at wileyonlinelibrary.com.]

the pure matrix response, with minimal fiber reinforcement effect. Thus, all modulus and hardness values were taken within these limits of penetration depth (200–400 nm). Figure 9 summarizes the findings from all the nano-indentation tests. The average elastic modulus and hardness values of the matrix in the autoclaved sample were 19% and 54% higher, respectively, than that observed in the LATP sample, which is in-line with the afore-mentioned DSC findings of much higher crystallinity in the autoclaved specimens. The measured values of elastic modulus and hardness of the PEEK matrix are in the same range as reported in a previous work.[24]

Results from SEM of Post-Test DCB Specimens

SEM micrographs of the post-test DCB samples were taken from areas approximately 25 mm from the pre-crack position. The crack surfaces as well as the cross sections of the samples were examined under SEM to observe the effect of the loading not just along the crack surface, but also through the thickness of the composite. Figure 10(a–f) shows the SEM micrographs of the crack surfaces of the autoclave and LATP processed samples. For autoclave samples, the unstable crack growth regions exhibited brittle failure of the matrix [Figure 10(a,b)] while, in stable fracture regions, the polymer showed high ductility, being drawn considerably locally [Figure 10(c,d)]. This difference in texture was the reason for the optical difference (lighter appear-

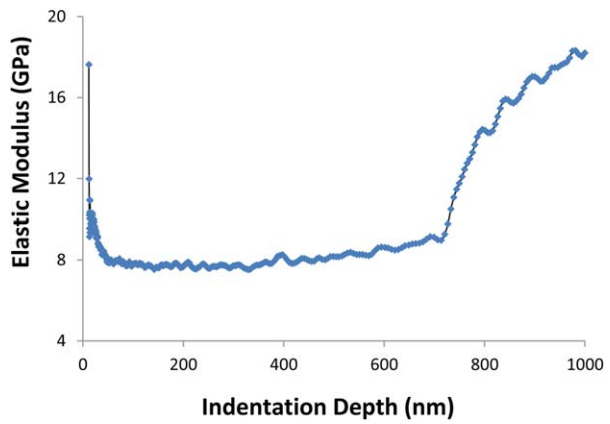

Figure 8. Variation of elastic modulus as a function of indentation depth in the AC sample (nano-indentation test). [Color figure can be viewed in the online issue, which is available at wileyonlinelibrary.com.]

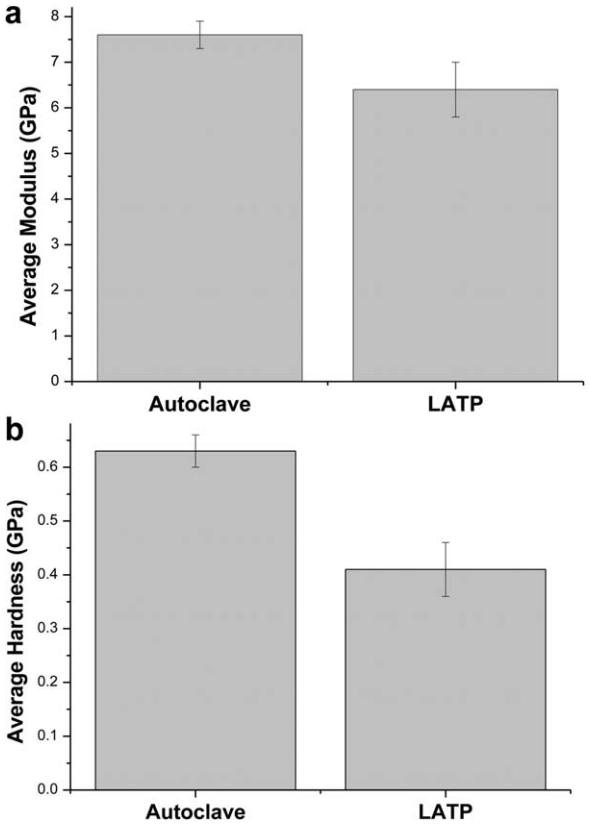

Figure 9. (a) Average elastic modulus and (b) average hardness of PEEK matrix in autoclave and ATP laminates over a penetration depth range of 200–400 nm.

ance of the stable region) shown in Figure 5(a). A transcrystalline interphase region is evident which is still attached to the fibers after the test. In the LATP sample [Figure 10(e,f)], clean fiber surfaces were visible indicating weak interfacial bonding, and the stable crack growth areas revealed micro-ductility which was not evident in the unstable crack propagation areas. The overall ductility displayed by the LATP specimen surface was much higher than for the autoclaved surface.

The cross sections of the samples after DCB tests were mounted, ground, polished, and examined under SEM, the results of which are shown in Figure 11. For the autoclaved specimens, brittle crack propagation was evident along the under-surface of the inter-ply region parallel to the crack surface [Figure 11(a)], while for the LATP specimens, numerous debonded regions, which appear as voids, were observed not only in the inter-ply region but also within the interior of several plies beneath the crack (let us call this the "bulk material") [Figure 11(b)]. This indicates that in the autoclaved specimens, the bond was weaker than the bulk material and so plastic deformation and energy absorption were largely confined to the inter-ply region. In the LATP specimens, the bond was of a similar strength to the bulk material, and significant plastic deformation and energy absorption occurred within the bulk material before the two surfaces separated and the crack grew. By bringing the bulk material into play for energy absorption, the fracture toughness was significantly increased. We have already seen from the DSC and DMA results that the LATP specimens were less crystalline and tougher than the autoclaved

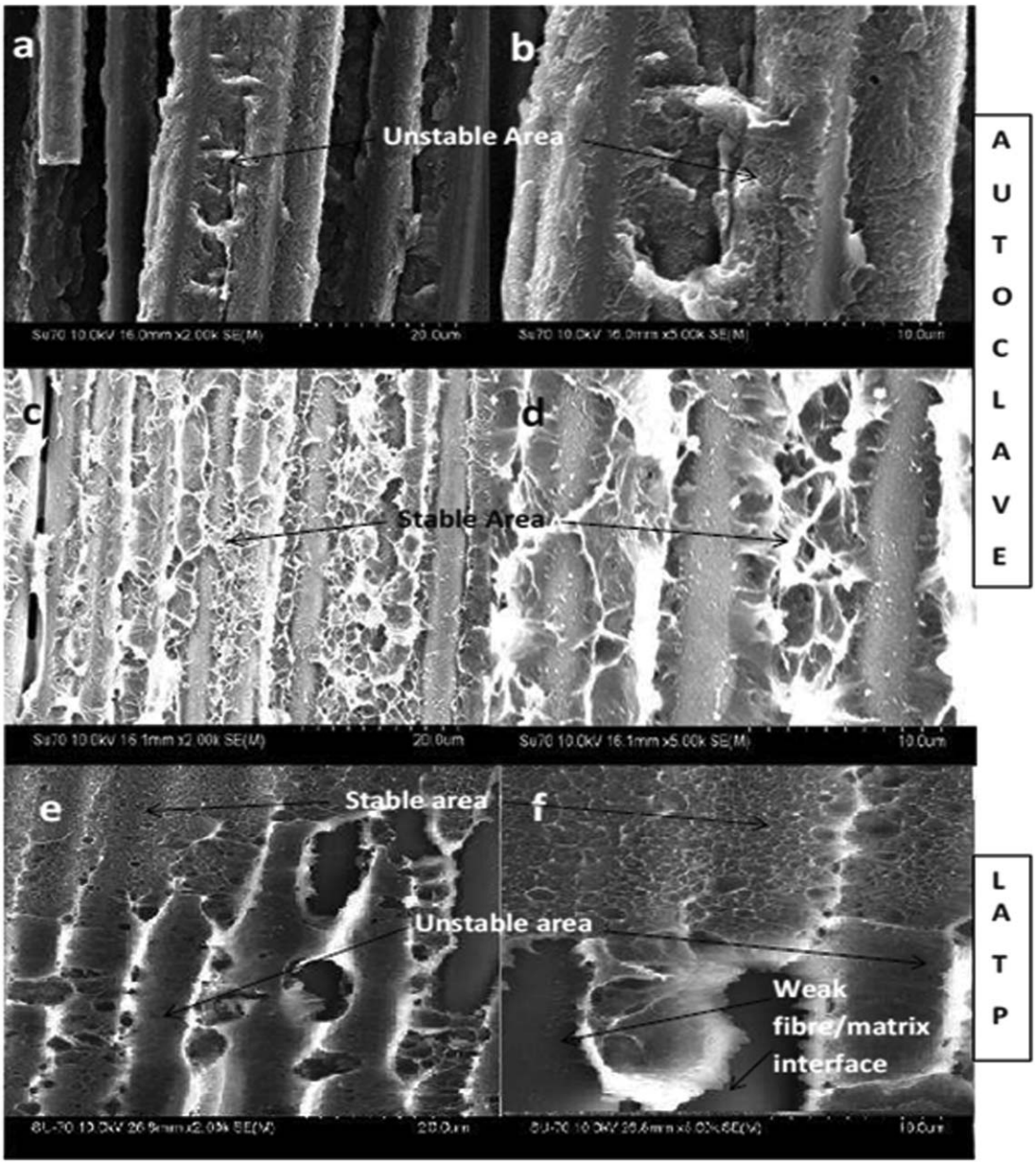

Figure 10. SEM micrographs of mode-I interlaminar fracture surface of autoclave and LATP composites: (a) and (b) brittle fracture in unstable crack growth region in autoclave sample; (c) and (d) ductile plastic deformation of the matrix in the stable crack growth area in autoclave sample; (e) and (f) transition between stable to unstable crack growth region in LATP sample.

specimens, while the DMA results also indicated that they were less stiff. Nano-indentation results indicated they were less hard. These properties allow the bulk material to plastically deform and absorb energy during the DCB tests, whereas in the autoclaved samples, the bulk material is more brittle so that plastic deformation does not occur within the plies, but only at the interply region of the crack.

DISCUSSION AND CONCLUSIONS

The work performed in this study found that the fracture toughness of the CF/PEEK composites produced by LATP was 60–80% higher than laminates produced by autoclave processing. However, LATP processed laminates displayed significantly lower stiffness and strength. The magnitude of the difference between autoclaved and LATP samples was surprising, but is at least partially explained by the lower crystallinity exhibited by the LATP (≈18%) compared to autoclave processed laminates (≈42%) and higher toughness of the matrix in the LATP laminate. In addition, SEM analysis of DCB specimens in-plane and through-thickness fracture surfaces indicated that there was considerable plastic deformation within the bulk material of the LATP specimen before the bond completely fails, thus bringing more material into play for energy absorption. This suggests that strength of the bond and the strength of the bulk material in the LATP specimens were of a similar magnitude. Another

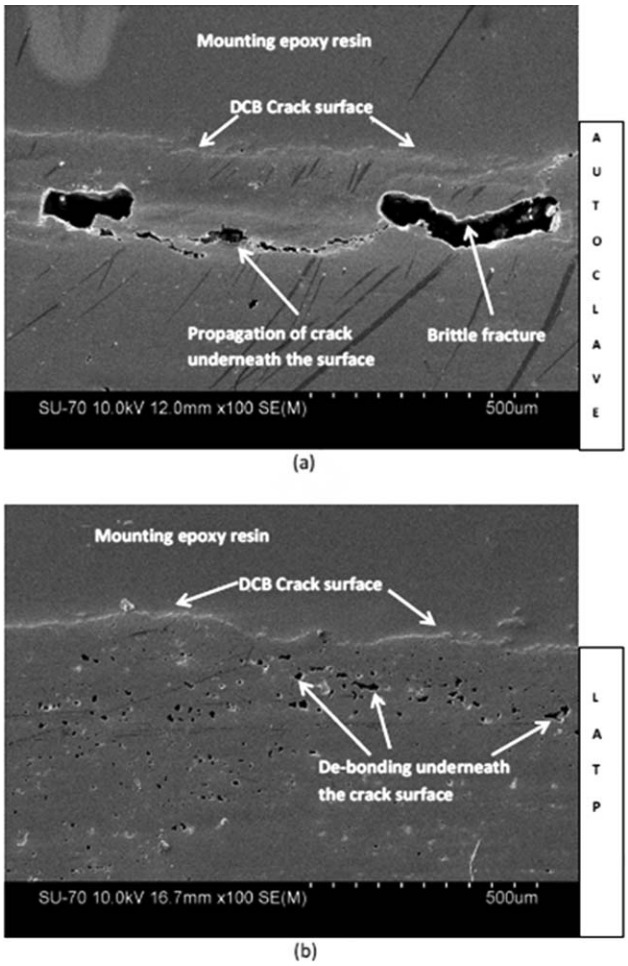

Figure 11. SEM micrographs of the cross sections of (a) autoclave and (b) LATP samples after DCB failure (samples mounted in epoxy).

contributing factor is that the crystallinity in the autoclaved specimen is higher than the optimum. As the baseline specimens, autoclave processed laminates were to have the optimum level of crystallinity, ≈35%, for good mechanical properties.[18] This was to be achieved by controlling the autoclave cooling rate (not a trivial exercise) to 2°C/min (this rate was estimated based on previous DSC analysis). However, post-processing analysis revealed a slightly higher than optimum crystallinity level (≈42%), yielding a slightly less tough laminate.

From the experimental results, the following conclusions can be drawn:

- The low crystallinity in the LATP specimens could be due to the high cooling rates in that process.
- Alternatively it could be that in the LATP process, the interior portion of plies is not fully heated above the melting point of PEEK, that is, unlike hot gas heating, the laser may be heating only a very thin portion of the bottom of the ply being laid down and top of the ply laid down during the last pass. In that case, the crystallinity of the prepreg would be carried forward into the final product, more or less unchanged.
- Further investigation is required to confirm which of these processes is responsible for the low crystallinity levels encountered. The LATP process thus appears to produce a very good quality bond between the plies but a low level of crystallinity in the bulk material, and low fiber–matrix adhesion.
- Clearly there is considerable scope for optimizing the LATP process, before the optimum balance between strength and toughness is achieved at favorable lay-down speeds.

ACKNOWLEDGMENTS

The authors wish to acknowledge Mr. Adrian McEvoy, the Department of Mechanical, Aeronautical and Biomedical Engineering, University of Limerick for help with the mechanical tests and Dr. Lekshmi Kailash, The Material and Surface Science Institute, University of Limerick for help with nano-indentation experiments. The authors would like to acknowledge Enterprise Ireland for providing financial support to conduct the current research project PROTHERM under grant number: CF/2010/ICComp2010-01. This work was also conducted under the framework of the Irish Government's Programme for Research in Third Level Institutions Cycle 5, with the assistance of the European Regional Development fund.

REFERENCES

1. Steyer, M.; Dubratz, M.; Schütte, A.; Wenzel, C.; Brecher, C. *JEC Compos. Mag.* **2009**, *47*, 39.
2. Schledjewski, R. *Plast. Rub. Comp.* **2009**, *38*, 379.
3. Tierney, J. J.; Quirico, S.; Eduljee, R. F.; Gillespie, J. W., Jr. In development of material quality during the automated tow-placement process, American Society for Composites Thirteenth Technical Conference, Baltimore, MD, **1998**.
4. Tierney, J. J.; Heider, D.; Gillespie, J. W., Jr.; Shevchenko, N. B.; Fink, B. K. In Automated induction lamination (R.A.I.L) for high-volume production of carbon/thermoplastic laminates. Proceeding of the SAMPEACCE- DOE-SPE, Midwest Advanced Materials and Processing Conference, Sept 12–14, Dearborn, MI, 2000, p 393.
5. Agarwal, V.; Güçeri, S. I.; McCullough, R. L.; Schultz, J. M. *J. Thermoplast. Compos. Mater.* **1992**, *5*, 115.
6. Dara, P. H.; Loos, A. C. Thermoplastic matrix composite processing model, In Center for Composite Materials and Structures Report 1985, Virginia Polytechnic Institute and State University: Blacksburg, VA.
7. Mantell, S. C.; Springer, G. S. *J. Compos. Mater.* **1992**, *26*, 2348.
8. Lee, W. I.; Springer, G. S. *J. Compos. Mater.* **1987**, *21*, 1017.
9. Yang, F.; Pitchumani, R. *Polym. Eng. Sci.* **2002**, *42*, 424.
10. Yang, F.; Pitchumani, R. *J. Mater. Sci.* **2001**, *36*, 4661.
11. Gao, S. L.; Kim, J.-K. *Compos. Part A* **2001**, *32*, 763.
12. Gao, S. L.; Kim, J. K. *Compos. Part A* **2000**, *31*, 517.
13. Gao, S. L.; Kim, J. K. *Compos. Part A* **2001**, *32*, 775.
14. Li, T. Q.; Zhang, M. Q.; Zeng, H. M. *Compos. Part A* **2001**, *32*, 1727.
15. Vu-Khanh, T.; Frikha, S. J. *Thermoplast. Compos. Mater.* **1999**, *12*, 84.
16. Crick, R. A.; Leach, D. C.; Meakin, P. J.; Moore, D. R. *J. Mater. Sci.* **1987**, *22*, 2094.

17. Pistor, C. M.; Guceri, S. I. *J. Compos. Mater.* **1999**, *33*, 306.
18. Cogswell, F. N. In Thermoplastic Aromatic Polymer Composites; Cogswell, F. N., Ed.; Butterworth-Heinemann, Ltd.: Great Britain, **1992**, Chapter 4, p 92.
19. ASTM D5529, Standard test method for Mode I interlaminar fracture toughness of unidirectional fiber-reinforced polymer matrix composites, 2013.
20. Blundell, D. J.; Osborn, B. N. *Polymer* **1983**, *24*, 953.
21. Coban, O.; Bora, M. O.; Avcu, E.; Sinmazcelik, T. *Polym. Comp.* **2011**, *32*, 1766.
22. Gregory, J. R.; Spearing, S. M. *Compos. Sci. Technol.* **2005**, *65*, 595.
23. Hardiman, M.; Vaughan, T. J.; McCarthy, C. T. *Comput. Mater. Sci.* **2012**, *64*, 162.
24. Godara, A.; Raabe, D.; Green, S. *Acta Biomater.* **2007**, *3*, 209.